

Electronic States of Graphene Nanoribbons

L. Brey¹ and H. A. Fertig²

1. Instituto de Ciencia de Materiales de Madrid (CSIC), Cantoblanco, 28049 Madrid, Spain

2. Department of Physics, Indiana University, Bloomington, IN 47405

(Dated: March 23, 2022)

We study the electronic states of narrow graphene ribbons (“nanoribbons”) with zigzag and armchair edges. The finite width of these systems breaks the spectrum into an infinite set of bands, which we demonstrate can be quantitatively understood using the Dirac equation with appropriate boundary conditions. For the zigzag nanoribbon we demonstrate that the boundary condition allows a particle- and a hole-like band with evanescent wavefunctions confined to the surfaces, which continuously turn into the well-known zero energy surface states as the width gets large. For armchair edges, we show that the boundary condition leads to admixing of valley states, and the band structure is metallic when the width of the sample in lattice constant units is divisible by 3, and insulating otherwise. A comparison of the wavefunctions and energies from tight-binding calculations and solutions of the Dirac equations yields quantitative agreement for all but the narrowest ribbons.

PACS numbers: 73.22-f, 73.20-r, 73.23-b

I. INTRODUCTION

Improvements in the processing of graphite have made possible the isolation of two dimensional carbon sheets known as graphene [1]. The experimental observation of the quantum Hall effect in ribbons of this material, with widths in the micron [2] or submicron [3] range, indicates unambiguously the two dimensional character of the system. The possibility of gating and further processing such graphene sheets into multi-terminal devices has opened a new field of carbon-based nanoelectronics, where graphene nanoribbons could be used as connections in nanodevices.

The electronic properties of a nanometer scale carbon system depends strongly on its size and geometry [4, 5]. This is well known in the case of nanotubes, which are graphene sheets rolled into cylinders [6]. The geometry dependence is strongly influenced by the bipartite character of the graphene lattice. For carbon nanotubes the wrapping direction imposes different boundary conditions on the wavefunction in the different sublattices, which determines whether the system is semiconducting or metallic.

In this work we study the electronic states of graphene ribbons with different atomic terminations (Fig.1). Using tight-binding calculations, we show that the electronic properties depend strongly on the size and geometry of the graphene nanoribbons. We demonstrate that the electronic energies and states may be understood in terms of eigenvalues and eigenvectors of the Dirac Hamiltonian, which describes the physics of the electrons near the Fermi energy of the undoped material.

We now summarize our results. We find that for nanoribbons with zigzag edges, the correct boundary condition is for the wavefunction to vanish on a single sublattice at each edge. In this case the nanoribbon has confined electronic states with wavefunctions that involve sites on both sublattices, and is extended across the system. In addition, there are surface states strongly lo-

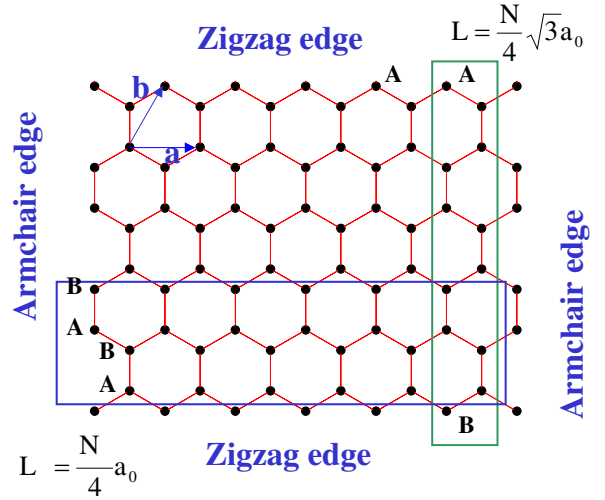


FIG. 1: (Color online) The lattice structure of a graphene sheet. The primitive lattice vectors are denoted by \mathbf{a} and \mathbf{b} . Top and bottom are zigzag edges, left and right are armchair edges. Atoms enclosed in the vertical (horizontal) rectangle represent the unit cell used in the calculation of nanoribbons with zigzag (armchair) edges. The length of the nanoribbons, L , as function of the number of atoms, N , in the unit cell is also indicated.

calized near the edges which are non-vanishing only on a single sublattice. For armchair edges, the appropriate boundary condition is for the wavefunction to vanish on both sublattices at the edges. This can be achieved by admixing states from both Dirac points. In this case we find that the electronic structure depends critically on the nanoribbon width, with the system being metallic for nanoribbons of width $L = 3Ma_0$, where M an integer and a_0 the graphene lattice constant, and insulating otherwise.

II. MODEL HAMILTONIAN

In graphene the carbon atoms crystallize in a honeycomb structure whose primitive lattice vectors are $\mathbf{a} = a_0(1, 0)$ and $\mathbf{b} = a_0(1/2, \sqrt{3}/2)$. The lattice is bipartite and there are two atoms per unit cell, denoted by A and B, located at $(0, 0)$ and at $\mathbf{d} = a_0(0, 1/\sqrt{3})$. In the simplest model, the carriers move in the x - y plane by hopping between the p_z orbitals of the carbon atoms. A tight-binding model with only nearest neighbor hopping t leads to a Hamiltonian with Dirac points at the six corners of the Brillouin zone, only two of which are inequivalent. We take these to be $\mathbf{K} = \frac{2\pi}{a_0}(\frac{1}{3}, \frac{1}{\sqrt{3}})$ and $\mathbf{K}' = \frac{2\pi}{a_0}(-\frac{1}{3}, \frac{1}{\sqrt{3}})$. Wavefunctions can be expressed via the $\mathbf{k} \cdot \mathbf{P}$ approximation [7, 8] in terms of envelope functions $[\psi_A(\mathbf{r}), \psi_B(\mathbf{r})]$ and $[\psi'_A(\mathbf{r}), \psi'_B(\mathbf{r})]$ for states near the \mathbf{K} and \mathbf{K}' points, respectively, which may be combined into a 4-vector $\Psi = (\psi_A, \psi_B, -\psi'_A, -\psi'_B)$ [9]. This satisfies a Dirac equation $H\Psi = \varepsilon\Psi$, with

$$H = \gamma a_0 \begin{pmatrix} 0 & -k_x + ik_y & 0 & 0 \\ -k_x - ik_y & 0 & 0 & 0 \\ 0 & 0 & 0 & k_x + ik_y \\ 0 & 0 & k_x - ik_y & 0 \end{pmatrix}, \quad (1)$$

where $\gamma = \sqrt{3}t/2$. Note that \mathbf{k} denotes the separation in reciprocal space of the wavefunction from the \mathbf{K} (\mathbf{K}') point in the upper left (lower right) block of the Hamiltonian.

The bulk solutions of Hamiltonian (1) are well-known [7]. The eigenstates retain their valley index as a good quantum number and the wavefunctions, with energies $\varepsilon = \pm\gamma a_0|\mathbf{k}|$, may be written as $[e^{i\mathbf{k}\mathbf{r}}e^{-i\theta_{\mathbf{k}}/2}, \mp e^{i\mathbf{k}\mathbf{r}}e^{i\theta_{\mathbf{k}}/2}, 0, 0]$ for the \mathbf{K} valley, and $[0, 0, e^{i\mathbf{k}\mathbf{r}}e^{i\theta_{\mathbf{k}}/2}, \pm e^{i\mathbf{k}\mathbf{r}}e^{-i\theta_{\mathbf{k}}/2}]$ for the \mathbf{K}' valley. Here $\theta_{\mathbf{k}} = \arctan k_x/k_y$. Note that a solution to the Dirac equation $(\psi_A, \psi_B, -\psi'_A, -\psi'_B)$ with energy ε has a particle-hole conjugate partner [10] $(\psi_A, -\psi_B, -\psi'_A, \psi'_B)$ with energy $-\varepsilon$. Because of this, the eigenstates of Eq.1 must be normalized on each sublattice separately [9]: $\int d\mathbf{r}[|\psi_\mu(\mathbf{r})|^2 + |\psi'_\mu(\mathbf{r})|^2] = 1/2$, for $\mu = A, B$.

III. ZIGZAG NANORIBBONS

The geometry of a nanoribbon with zigzag edges is illustrated on the top and bottom edges of Fig. 1. It is interesting to note that the atoms at each edge are of the same sublattice (A on the top edge of Fig. 1 and B on the bottom edge). In Fig. 1 we also show the unit cell used in the tight-binding calculations of the zigzag ribbons, containing $N/2$ A-type atoms that alternate along the unit cell with $N/2$ B-type atoms. The total width of the nanoribbon is $L = \frac{N}{4}\sqrt{3}a_0$. We impose periodic boundary conditions along the direction parallel to the edge. In our discussions we will assume that the edges lie along the \hat{y} direction, so in the discussion of the zigzag nanoribbons, the coordinate axes in Fig. 1 will be

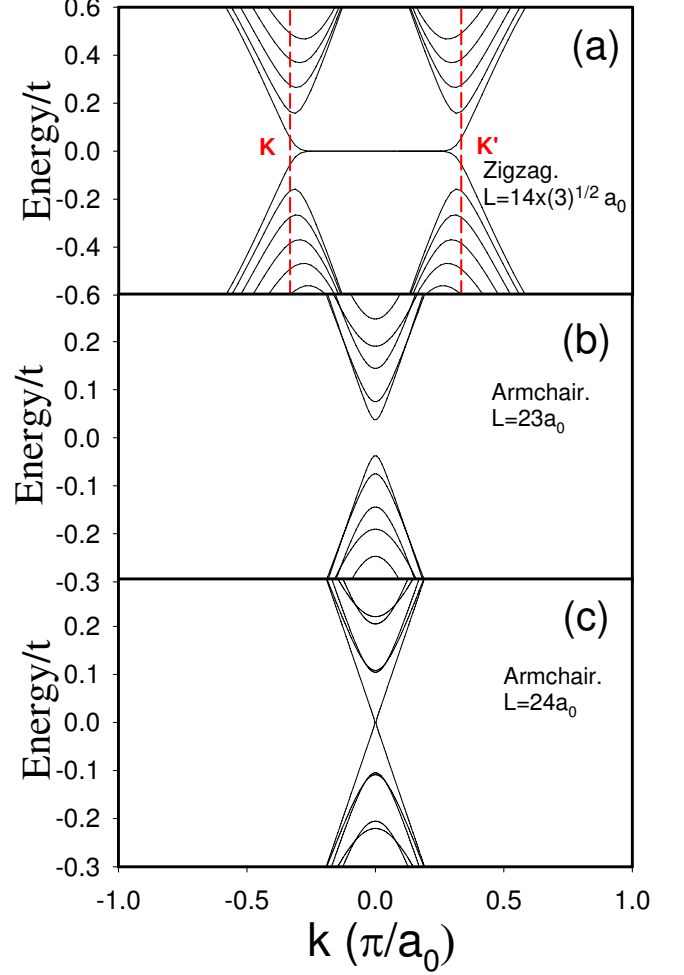


FIG. 2: (Color online) Examples of energy bands for a graphene nanoribbon with periodic boundary conditions in one direction. k is the wavevector parallel to the nanoribbon edge, measured with respect to the center of the Brillouin center. (a) Ribbon terminated in zigzag edges with 56 atoms in the unit cell. The dispersionless states correspond to confined surface states. The band structures of insulating and metallic armchair nanoribbons are plotted in (b) and (c) respectively.

rotated by 90° , and the eigenstates are proportional to e^{iky} . In Fig. 2 we plot an example of the band structure of a nanoribbon with zigzag edges. The finite width of the ribbon produces confinement of the electronic states near the Dirac points. In Fig. 3 we plot the energy of the first three confined states, at $k = K_y$, as a function of the nanoribbon width. The two bands of dispersionless localized surface states [11, 12, 13, 14] that occur between K_y and K'_y in Fig. 2(a) are also affected by the finite width: they admix, and the two bands are slightly offset from zero. The dependence of the electronic states on the width of the nanoribbon may be understood in terms of eigenstates of the Dirac Hamiltonian with appropriate boundary conditions: setting the wavefunction to zero on the A sublattice on one edge, and on the B sublattice

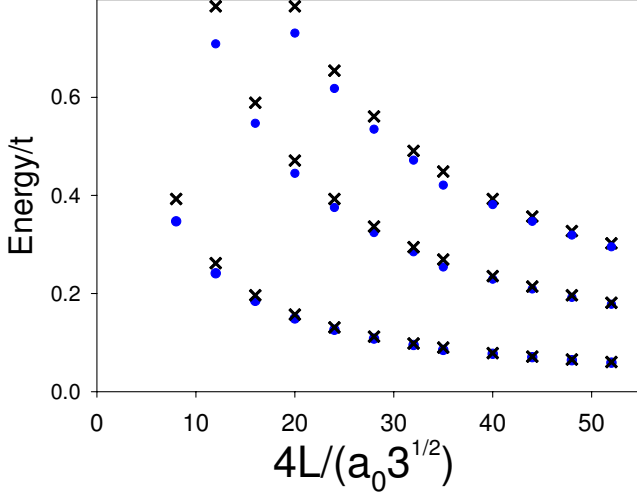


FIG. 3: (*Color online*) Calculated confined state energies at a Dirac point versus the nanoribbon width, in a zigzag nanoribbon. The dots are tight binding results, and the crosses are the results of the $\mathbf{k} \cdot \mathbf{P}$ approximation.

for the other. We can understand the lines of vanishing wavefunction to be lattice sites that would lie just beyond the edges if bonds had not been cut to form them.

For the continuum description, we begin by rotating the wavevectors in Eq. 1, $k_x \rightarrow k_y$, $k_y \rightarrow -k_x$ so that the zigzag edge lies along the \hat{y} , and our wavefunctions exist in the space $0 < x < L$. Translational invariance in the \hat{y} direction guarantees the wavefunctions can be written in the form $\psi_\mu(\mathbf{r}) = e^{ik_y y} \phi_\mu(x)$. For the \mathbf{K} (\mathbf{K}') valley the wavefunctions obey

$$\begin{aligned} (-\partial_x^2 + k_y^2) \phi_B(x) &= \tilde{\varepsilon}^2 \phi_A(x) \\ (-\partial_x^2 + k_y^2) \phi_A(x) &= \tilde{\varepsilon}^2 \phi_B(x) \end{aligned} \quad (2)$$

with $\tilde{\varepsilon} = \varepsilon/(\gamma a_0)$. It is easy to see if one solves the equations for ϕ_B and ϕ'_A , the remaining wavefunctions are determined by

$$\begin{aligned} \tilde{\varepsilon} \phi_B &= (i\partial_x - ik_y) \phi_A \\ \tilde{\varepsilon} \phi'_A &= (-i\partial_x + ik_y) \phi'_B. \end{aligned} \quad (3)$$

The general solutions of Eq.(2) have the form

$$\phi_\mu(x) = A e^{zx} + B e^{-zx}, \quad (4)$$

with $z = \sqrt{k_y^2 - \tilde{\varepsilon}^2}$, which can be real or imaginary.

For the zigzag nanoribbon, we meet the boundary condition for each type of wavefunction separately:

$$\phi_A(x=0) = \phi'_A(x=0) = \phi_B(x=L) = \phi'_B(x=L) = 0. \quad (5)$$

These conditions leads to a transcendental equation for the allowed values of z ,

$$\frac{k_y - z}{k_y + z} = e^{-2Lz}. \quad (6)$$

Eq.(6) supports solutions with real values of $z \equiv k$ for $k_y > k_y^c = 1/L$, which correspond to the surface states.

These have energies $\pm \sqrt{k_y^2 - k^2}$, and are linear combinations of states localized on the left and right edges of the ribbon. For large values of k_y , $k \rightarrow k_y$ and the surface states become decoupled. For $k_y < 0$ there are no states with real z that can meet the boundary conditions, so surface states are absent. For values of k_y in the range $0 < k_y < k_y^c$, the surface states are so strongly admixed that, as we show below, they are indistinguishable from confined states.

For pure imaginary $z = ik_n$, the transcendental equation becomes

$$k_y = \frac{k_n}{\tan(k_n L)}, \quad (7)$$

and for each solution k_n there are two confined states with energies $\tilde{\varepsilon} = \pm \sqrt{k_n^2 + k_y^2}$ and wavefunctions

$$\begin{pmatrix} \phi_A \\ \phi_B \end{pmatrix} = \begin{pmatrix} \sin(k_n x) \\ \pm \frac{i}{\tilde{\varepsilon}} (-k_n \cos(k_n x) + k_y \sin(k_n x)) \end{pmatrix}. \quad (8)$$

Here the index n indicates the number of nodes of the confined wavefunction. Interestingly, for values of k_y larger than k_y^c , Eq.(7) does not support nodeless solutions, indicating the existence of surface states in this region of reciprocal space. The critical value k_y^c is the momentum where the lowest energy solution of the transcendental Eq. 6 changes from pure real to pure imaginary, and the energy is equal to $\pm |k_y^c|$.

In order to analyze the accuracy of the $\mathbf{k} \cdot \mathbf{P}$ approximation for describing the electronic properties of carbon nanoribbons, in Fig. 3 we plot the energies of the three lowest confined states of a zigzag nanoribbon as a function of its width, both from the tight-binding approach and from our solutions to the Dirac equation. It is apparent that the two approaches match quite well, even for rather small widths ($\sim 35\text{\AA}$).

In Fig. 4 we plot the squared wavefunction for the lowest energy state of a zigzag nanoribbon as obtained in the tight binding approach. Fig. 4(a) corresponds to $k_y = 0$ ($k = -2\pi/3a_0$ with respect the center of the Brillouin zone), and Fig. 4(b) to $k_y = 0.02 \times 2\pi/3a_0$. The first case corresponds to a nodeless confined state, and we find the wavefunction is described nearly perfectly by Eq.(8), whereas the second case is the expected linear combination of surface state wavefunctions that decay exponentially from the edges as $\exp(-kx)$.

IV. ARMCHAIR NANORIBBONS

The geometry of a nanoribbon with armchair edges is illustrated on the left and right edges of Fig. 1, along with the unit cell used in the corresponding tight binding calculations. In this orientation the width of the nanoribbon is related to the number of atoms in the unit cell through

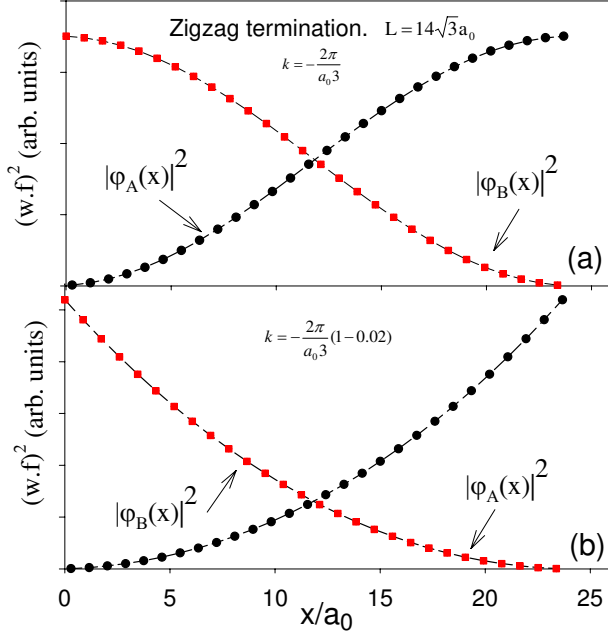


FIG. 4: (*Color online*) Squared wavefunction for the state closest to zero energy for a zigzag nanoribbon, as obtained from tight binding calculations. The width of the ribbon is $L = 14\sqrt{3}a_0$. (a) $k = -2\pi/3a_0$, and (b) $k = (-2\pi/3a_0)(1 - 0.02)$. Both are measured from the center of the Brillouin zone.

the expression $L = \frac{N}{4}a_0$. Here the edge runs along the \hat{y} direction, and no rotation of the figure is needed to represent our calculations.

The electronic properties of armchair nanoribbons depend strongly on their width. In Fig. 2(b) and (c) we plot two examples of band structures of armchair nanoribbons. One sees that in the latter figure there is a Dirac point, leading to metallic behavior for a non-interacting model, whereas the former is a band insulator. In general we find that armchair nanoribbons of width $L = 3Ma_0$, with M integral, are metallic, whereas all the other cases are insulators. The energy of the confined states also behave in a discontinuous way with respect to the width of the ribbon. In Fig. 5 we plot the energy of the lowest (squared) energy confined states at the center of the Brillouin zone as a function of the nanoribbon width. In the inset of this figure we see that the separation in energy between confined states is also strongly dependent on the number of atoms in the unit cell.

As in the case of the zigzag nanoribbons this behavior may be understood in terms of eigenstates of the Dirac Hamiltonian with the correct boundary conditions. In Fig. 1 one may see that the termination consists of a line of A-B dimers, so it is natural to have the wavefunction amplitude vanish on both sublattices at $x = 0$ and $x = L$.

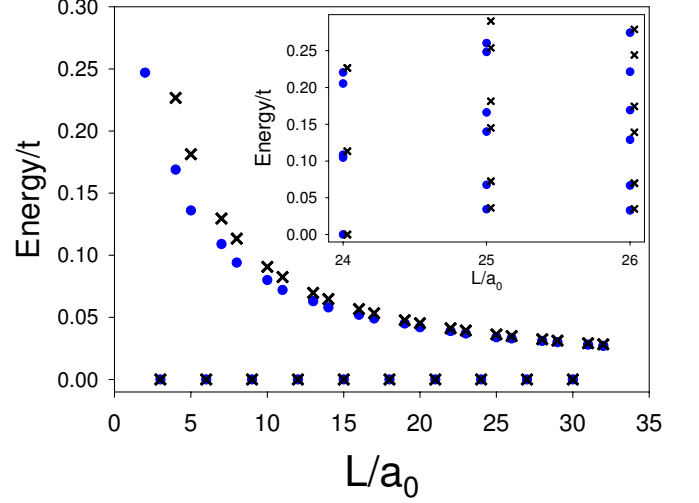


FIG. 5: (*Color online*) Calculated lowest energy confined states at the center of the Brillouin zone versus the nanoribbon width, for an armchair nanoribbon. The dots correspond to the tight binding results and the crosses are the results of the $\mathbf{k} \cdot \mathbf{P}$ approximation. In the inset we plot the six lowest energy confined states for three different widths. The $\mathbf{k} \cdot \mathbf{P}$ results are slightly shifted to the right for clarity. Note that for $L = 24a_0$ the $\mathbf{k} \cdot \mathbf{P}$ results are doubly degenerate.

To do this we must admix valleys, and require

$$\begin{aligned}\phi_\mu(x=0) &= \phi'_\mu(x=0) \\ \phi_\mu(x=L) &= \phi'_\mu(x=L) e^{i\Delta K L},\end{aligned}$$

with $\Delta K = \frac{2\pi}{3a_0}$. With these boundary conditions the general solutions of the Dirac equation are plane waves,

$$\phi_B(x) = e^{ik_n x} \quad \text{and} \quad \phi'_B(x) = e^{-ik_n x}. \quad (9)$$

The wavefunctions on the A sublattice may be obtained via Eq. 3. The wavevector k_n satisfies the condition

$$e^{2ik_n L} = e^{i\Delta K L}, \quad (10)$$

so that

$$2k_n L = \frac{2\pi}{3} j + 2\pi n, \quad (11)$$

with n an integer and $j = 0, \pm 1$, determined by

$$\frac{N}{4} = 3M + j \quad (12)$$

for an integer M . Thus for armchair nanoribbons the allowed values of k_n are

$$k_n = \frac{4}{N}\pi \left(n \pm \frac{j}{3} \right) \quad (13)$$

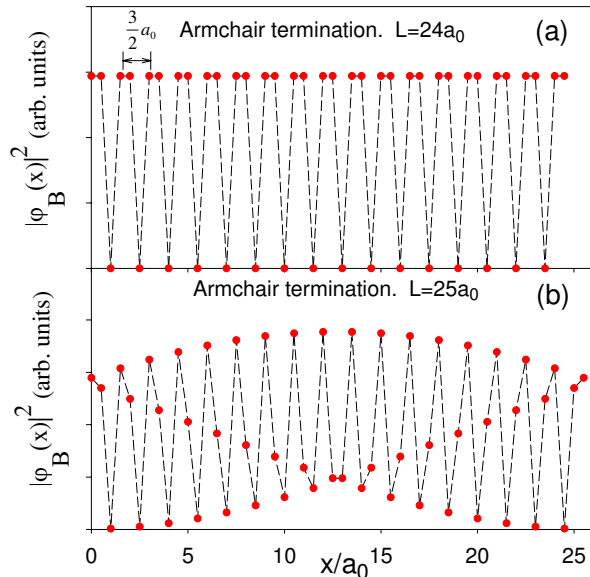


FIG. 6: (Color online) Squared wavefunction of the state with energy closest to zero for an armchair ribbon of width (a) $L = 24a_0$ and (b) $L = 25a_0$, as obtained from tight binding calculations.

with energies $\pm\sqrt{k_n^2 + k_y^2}$. Note that this is in contrast to the zigzag nanoribbon for which the allowed values of k_n depend on k_y . For a width that is a multiple of $3a_0$, the allowed values of k_n , $k_n = n4\pi/N$, create doubly degenerate states for $|n| \geq 0$, and allow a zero energy state when $k_y \rightarrow 0$. Nanoribbons of widths that are not multiples of three have nondegenerate states and do not include a zero energy mode. Thus these nanoribbons are band insulators. The quality of the $\mathbf{k} \cdot \mathbf{P}$ approximation for describing the electronic states of armchair nanoribbons is reflected in Fig. 5 where the energies of the confined states obtained by diagonalizing the tight binding

Hamiltonian and by solving Eq.(13) are compared. The quantitative agreement is apparent for all but the narrowest ribbons, where one does not expect the $\mathbf{k} \cdot \mathbf{P}$ to work well.

The admixing of different valley states to meet the boundary condition means that the wavefunction will oscillate with period $2\pi/\Delta K$ [9]. This behavior can explicitly be seen in Fig. 6, which illustrates the squared wavefunction from the tight binding calculation. The short oscillation in the wavefunctions has exactly the period expected for the valley mixing we introduced to meet the boundary conditions. In the case of Fig. 6(a), the ribbon is of width $L = 24a_0$ and $k_n = 0$, so that the energy is zero and there is no confinement effect on the form of the wavefunction. For a ribbon of width $L = 25a_0$ [Fig. 6(b)], k_n is non-zero and one sees a long-wavelength oscillation whose period is related to the value of k_n .

V. CONCLUSION

In this paper we studied eigenstates and eigenenergies of graphene nanoribbons using the Dirac equation with appropriate boundary conditions, and compared the results to those of tight binding calculations. We found that except for the narrowest ribbons, the agreement was quantitative. Zigzag nanoribbons support surface states which go to zero energy in the limit of wide ribbons, and can only be found in a k_y interval between the Dirac points. Armchair nanoribbons have no surface states, but in spite of their finite size they have zero energy states for appropriately chosen widths, so that the system oscillates between insulating and metallic behavior as the width changes. Our results show that the continuum description of graphene may be used in quantitative analysis of this system for all but the most narrow systems.

Acknowledgements. The authors thank F.Guinea and C.Tejedor for useful discussions. This work was supported by MAT2005-07369-C03-03 (Spain) (LB) and by the NSF through Grant No. DMR-0454699 (HAF).

-
- [1] K.S.Novoselov, A.K.Geim, S.V.Mozorov, D.Jiang, Y.Zhang, S.V.Dubonos, I.V.Gregorieva, and A.A.Firsov, *Science* **306**, 666 (2004).
 - [2] Y.Zhang, Y.-W. Tan, H.L.Stormer, and P.Kim, *Nature* **438**, 201 (2005).
 - [3] K.S.Novoselov, A.K.Geim, S.V.Mozorov, D.Jiang, M. I.V.Gregorieva, S.V.Dubonos, and A.A.Firsov, *Nature* **438**, 197 (2005).
 - [4] R.Saito, G.Dresselhaus, and M.S.Dresselhaus, *Physical Properties of Carbon Nanotubes* (Imperial College, London, 1998).
 - [5] L.Chico, M.P.López-Sancho, and M.C.Muñoz, *Phys.Rev.Lett.* **81**, 1278 (1998).
 - [6] A very general discussion of boundary conditions for nanotubes described by the Dirac equation may be found in E. McCann and V.I. Fal'ko, *cond-mat/0402373*.
 - [7] T.Ando, *J.Phys.Soc.Jpn.* **74**, 777 (2005).
 - [8] D.P.DiVincenzo and E.J.Mele, *Phys. Rev. B* **29**, 1685 (1984).
 - [9] L.Brey and H.A.Fertig, *cond-mat/0602505*.
 - [10] S.Ryu and Y.Hatsugai, *Phys. Rev. Lett.* **89**, 077002 (2002).
 - [11] M.Fujita, K. Wakabayashi, K.Nakada, and K.Kusakabe, *J.Phys.Soc.Jpn.* **65**, 1920 (1996).
 - [12] K.Wakabayashi, *Carbon Bases Magnetism*. (Elsevier, 2006), chap. Electric and Magnetic Properties of Nanographites.
 - [13] M.Ezawa, *Phys.Rev.B* **73**, 045432 (2006).
 - [14] N.M.R.Peres, F.Guinea, and A.H.Castro-Neto, *cond-mat/0512091*.